Archives of Environmental Protection
Vol. 50 no. 1 pp. 95–109

PL ISSN 2083-4772
DOI:10.24425/aep.2024.149436

Analysis of cold island effect in city parks from the perspectives of maximum and cumulative values – a case study of Xi'an City

Yao Zhang, Qian Wang*, Yaqian Kong, Jing Quan, Yuxin Zhang, Yongjian Zhang

Shaanxi University of Science and Technology, China

* Corresponding author's e-mail: qianwang_11@163.com

Keywords: park cooling island, land surface temperate, buffer analysis, urban planning, Xi'an City

Abstract: The continuous process of urbanization and climate change has led to severe urban heat island (UHI) effects. Constructing parks with cooling capabilities is considered an effective measure to alleviate UHI effects. However, most studies only quantify the cooling effect from a maximum value perspective, lacking a measure of temperature diffusion in space. This study combines the perspectives of maximum value and accumulation to define a cold island index, quantifying the cooling effect of 40 urban parks in the main urban area of Xi'an city. The results show that, on average, urban parks can reduce the surrounding environment by approximately 2.3°C, with a cooling range of about 127.1ha, which is three times the park area. Different factors drive the measurement of the cooling effect using different cold island indexes, but all indexes are highly correlated with green space area. There are significant differences in the cooling effect among different types of parks, and overall, ecological parks have the best cooling effect. The directional spread of internal cold islands in parks is most related to park shape, while external spread is related to surrounding green spaces. The research results have practical value in the construction of parks with cooling effects and the sustainable development of cities in urban planning processes.

Introduction

Since the reform and opening-up, China's urbanization process has been advancing comprehensively. By the end of 2022, China's urbanization rate reached 65.22%, surpassing the global average. This process entails the conversion of vast natural and semi-natural land coverage areas into impermeable surfaces such as buildings and roads, resulting in changes in the thermal properties of urban land surfaces (Wu, Zhong et al. 2022). Coupled with intense human activities, the Urban Heat Island (UHI) effect emerges. Elevated surface temperatures are a prominent characteristic, with temperatures in urban areas significantly higher than those in surrounding suburbs. The UHI effect exacerbates energy consumption, increases air pollution, leads to localized natural disasters, and directly or indirectly harms the physical health of urban residents, impacting the sustainable development of cities. Therefore, against the backdrop of global climate change, the UHI effect has become an urgent and crucial issue in urban ecology (Algretawee at al. 2019).

In order to alleviate the UHI effect, various studies have found that the surface temperature is significantly affected by geographical location, climate type, and landscape configuration. Among them, urban blue-green space configuration can effectively absorb the energy of solar radiation. As a natural-based solution, due to its high efficiency and environmental friendliness, the construction of blue-green space in urban areas has been widely recommended to alleviate the UHI effect (Hong et al. 2022). As the most common blue-green space configuration in urban ecosystems, urban parks are characterized by high vegetation coverage and abundant water resources, which can play a significant role in cooling, especially in urban centers where the UHI effect is prominent, significantly reducing the surface temperature of the surrounding environment (Zhou et al. 2022). Therefore, the study on the mitigation of the UHI effect in urban parks is currently a hot topic.

At present, a large number of studies have been conducted from various perspectives on the cooling effect of parks, selection of influencing factors, and the planning of urban parks based on the research idea of quantifying the cooling effect (Li et al. 2022). In terms of quantifying the cooling effect of parks, some scholars define the difference between the average surface temperature inside and around the park as the park's cooling island intensity (Anjos and Lopes 2017), and calculate the cooling benefit of the park by calculating the ratio of the effective cooling range of the park to the surface temperature inside the park, using the surface temperature

as a variable (Ruochen et al. 2022). Some scholars have introduced the variable of spatial cooling distance to establish a buffer zone for analysis, and obtained the distance of the buffer zone where the temperature difference from the park boundary to the ground surface is less than 0.1℃, defining it as the spatial range where the park can significantly affect the ground surface temperature, namely the maximum cooling island distance. However, the cold island indicators proposed in previous studies, whether based on surface temperature or cooling distance are simple to calculate and have certain value. Despite differences in algorithms, these indicators are designed and calculated based on the perspective of maximum value. The change in surface temperature around the park is a continuous process, meaning that the cooling effect of the park is not spatially discrete. Considering only the maximum value to measure the cooling effect may lead to certain deficiencies in the planning and design process of urban parks (Wu, Li et al. 2019). The reasons are as follows: Firstly, the diffusion of the park's cool island effect in space is continuous and non-linear. The use of the maximum value angle as a cool island indicator cannot fully describe the spatial distribution of the cooling effect of the park. Secondly, there are significant differences in the cooling effects of parks with different landscape compositions and configurations in space (Peng et al. 2021). Even if the maximum cool island distance remains the same, the cool island fitting curve (LST-distance) may vary greatly. This implies that different parks with the same maximum value angle cool island indicator may have different cooling effects, which cannot be measured by the maximum value angle cool island indicator (Gao et al. 2022). In conclusion, the focus of this study is on how to optimize the quantification of the cooling effect of parks to enhance the comprehensiveness of measuring the cooling effect. To make the research more reasonable, there are limitations to solely using the maximum value angle as a cool island indicator when quantifying the cooling effect of parks. Therefore, this paper introduces the concept of definite integration in mathematics and cleverly combines the cool island cooling model with definite integration to obtain a park cool island effect indicator from the perspective of spatial accumulation angle. By combining both the maximum value and accumulation angles, the cooling effect of parks can be comprehensively described (Yao et al. 2022).

In terms of selecting factors that influence parks, it is well known that the relationship between landscape composition-including parameters such as park area, green spaces, and water bodies - and the urban heat island effect is closely linked. Furthermore, landscape configuration, another important characteristic of parks, has been identified by scholars as a significant factor affecting the cooling effect of parks through the establishment of simultaneous equation models (Liao et al. 2023). Therefore, this paper comprehensively considers both the landscape composition and landscape configuration factors when selecting influencing factors. It is worth noting that these characteristic factors can be adjusted and changed through rational planning and design, enabling parks to optimize their cooling effect and other services. In the planning of urban parks, scholars have considered the cooling effect of parks from the perspectives of regional scale and connectivity. They have developed a model called combined cool islands, which involves the elements of area (cool island sources), network (cool island connectivity), and points (cool island spaces). This model enhances the connectivity of cool islands at three levels to optimize the spatial distribution of cool sources and alleviate the urban heat environment effects(Qian and Li 2023, Qiu et al. 2023). Currently, the evaluation of parks' cooling effects mainly relies on indicators of cooling intensity in specific parks and limited datasets. Research on multiple parks also often uses park area as the criterion for

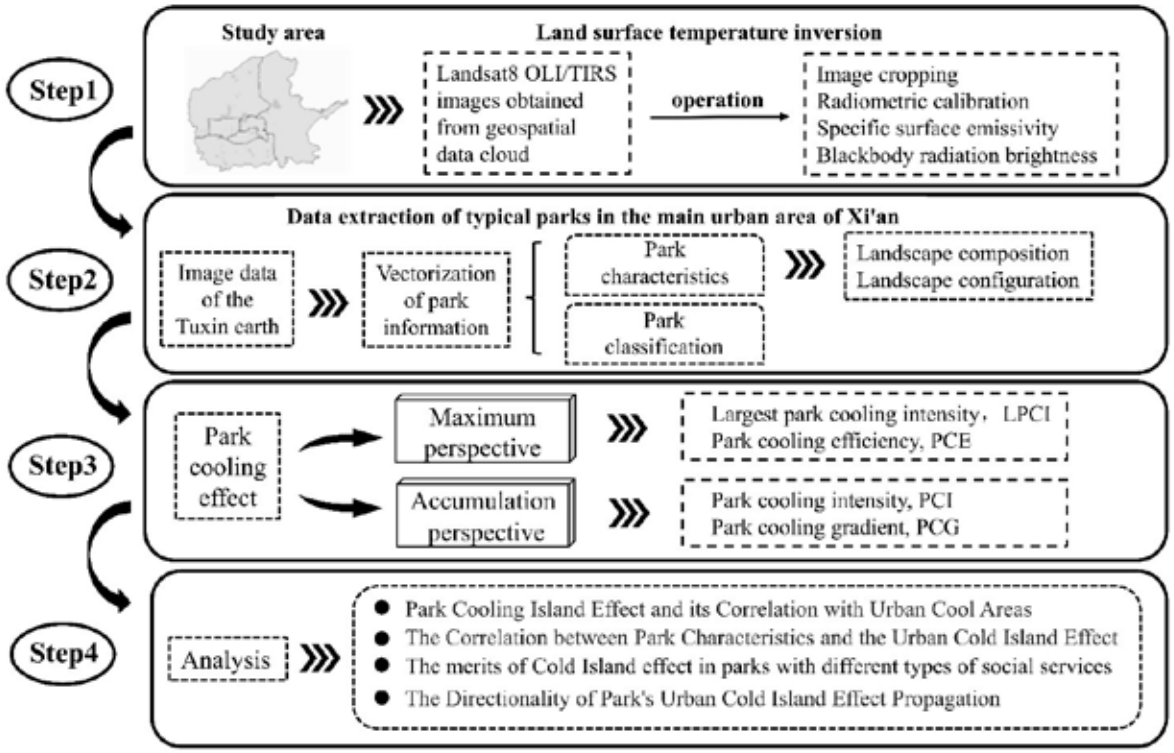

Figure 1. Research flow chart.

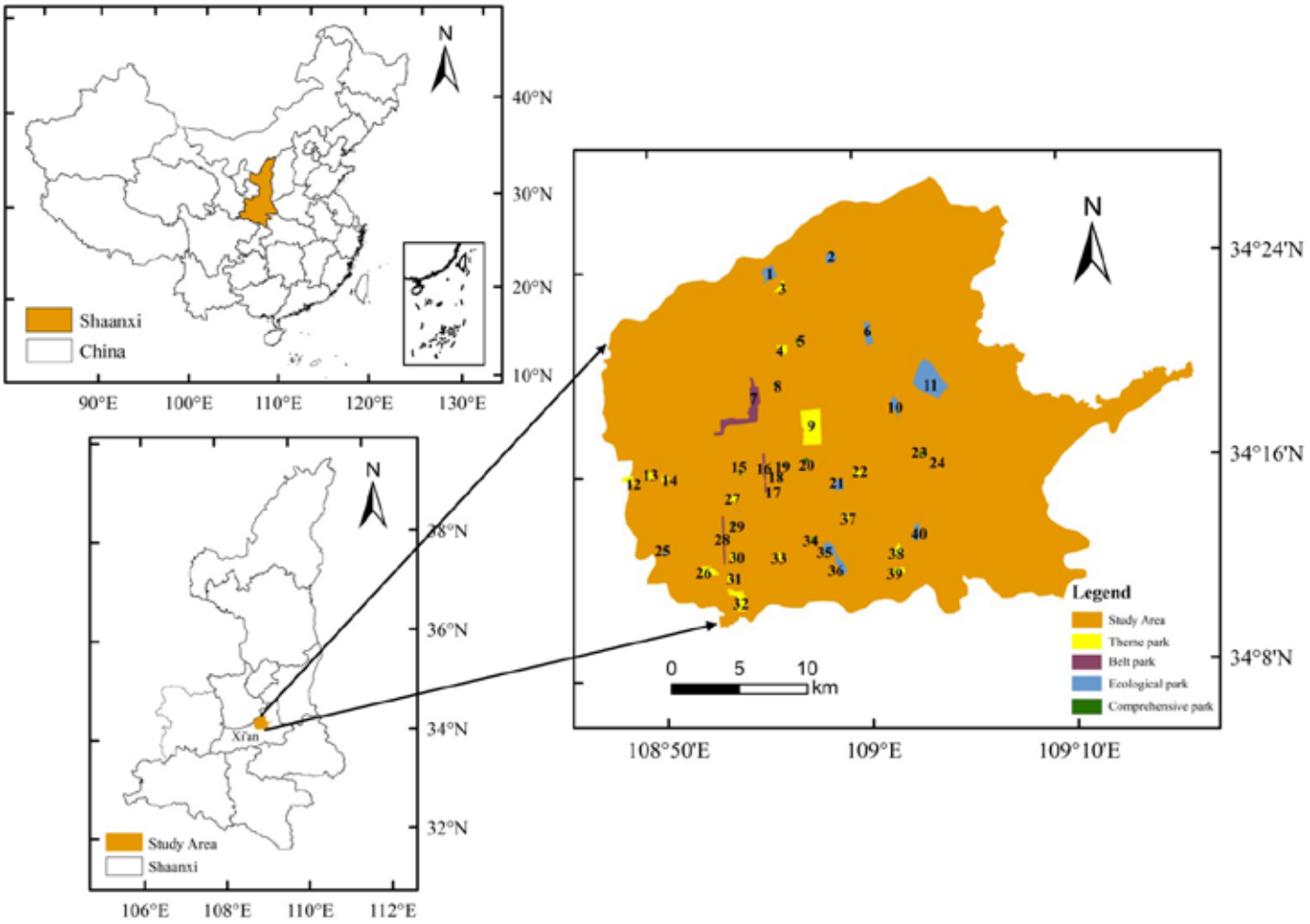

Figure 2. Location of the study area and distribution of 40 urban parks.

classification, with little consideration for the differences in the cooling effects of different park categories. Therefore, this study divides parks into different social service types and examines the advantages and disadvantages of different types of parks in terms of their cooling effects. This will provide data support for designing and planning parks that cater to different social needs in the future.

Xi'an is renowned as one of the most prominent "heat island cities" in China, and the only one in the northwest region (Gao, et al. 2020). Rapid urbanization, coupled with effects of climate change, and improper urban construction practices, has exacerbated severe urban heat pollution and placed unprecedented pressure on the local environment (Zhu, et al. 2019). To improve the urban environment, the Xi'an municipal government has systematically undertaken the construction of urban parks in the central urban area, aiming to enhance environmental resilience. Consequently, this study focuses on various urban parks within Xi'an central urban area, augmenting data on the cooling effects of parks by integrating various cool island effect indicators. Specifically, this research encompasses the following aspects: (1) Quantifying Park cooling effects based on maximum values and accumulations; (2) Identifying the main factors that influence park cooling effects; (3) Comparing cooling effects among parks of different categories; and (4) Describing the directional propagation of park cool islands. The research findings can provide scientific basis for urban planners on how to design future urban parks to mitigate the urban heat island effect. It also provides an integrated analysis platform to explore the relationship between ecosystem services and human well-being.

Materials and methods

Fig. 1 illustrates the research framework of this paper. Firstly, Landsat remote sensing data is used to retrieve the land surface temperature of Xi'an city through atmospheric correction method and analyze the spatial distribution characteristics of the thermal environment in Xi'an. Secondly, using LocaSpace Viewer satellite imagery data, characteristic parameters of typical parks in the central urban area are obtained, and different types of parks are classified according to the Chinese urban green space classification standard. Thirdly, park buffer zones are set up, and a function model of land surface temperature-distance is established to measure the cooling effects of parks from the perspectives of maximum values and accumulations. Subsequently, based on Pearson correlation analysis, the driving factors of park cooling effects are estimated under different evaluation criteria. Finally, using hot and cold spot analysis and standard deviation ellipse method, the advantages, disadvantages, and directional propagation of cooling effects in different types of parks are analyzed. The research data and specific methods are presented below.

Study area

As the capital city of Shaanxi Province and a core city in the Guanzhong Plain urban agglomeration, Xi'an is a world-renowned historical city. It is located in the central part of the Guanzhong Plain, with geographical coordinates ranging from 107°40'E to 109°49'E and from 33°42'N to 34°45'N. Encompassing an area of 1.08×10^5 km^2, it maintains an average elevation of 400 meters above sea level. The climate exhibits characteristics of a warm temperate semi-humid continental monsoon climate, marked by distinct four seasons, featuring hot and rainy summers, and cold and dry winters. The annual average temperature is 13.7℃, with the lowest temperature in January averaging -1.2℃ and the highest temperature in July averaging 26.6℃. The annual average precipitation is 783mm. In the past 20 years, Xi'an has undergone rapid urbanization, with the resident population increasing from 7.41 million in 2000 to 12.95 million in 2020, and the urbanization rate increasing from 42.1% to 79.5% (Sun et al. 2023). This study focuses on the six main urban areas in Xi'an, as shown in Fig. 2, with a total area of approximately 688km^2.

As of 2021, there are 132 registered urban parks in Xi'an, and the urban green coverage rate has reached 42.5%. In this study, the boundaries of urban parks were manually interpreted, and the characteristic parameters of 40 urban parks in the main urban area of Xi'an were extracted using LocaSpace Viewer. The park areas range from 1.5ha to 425.2ha, with an average area of 58.1ha. According to the "Classification Standard for Urban Green Spaces in China" (CJJ/T85-2022), the 40 major urban parks in the main urban area of Xi'an are classified into four types based on their social functions: comprehensive parks (11), ecological parks (10), theme parks (16), and band-shaped parks (3), as shown in Table 1.

Data sources

The Landsat 8 satellite is equipped with an Operational Land Imaging Instrument (OLI) and Thermal Infrared Sensor (TIRS), comprising 11 bands. Among these bands are two thermal infrared bands utilized for retrieving land surface temperature data. Previous studies have shown that land surface temperature retrieved from remote sensing images can effectively quantify the urban heat island effect and its relationship with urban landscape characteristics (Huang and Wang 2019). Therefore, in this study, Landsat 8 OLI/TIRS images (strip number 127, row number 36), collected from the Geospatial Data Cloud (http://www.gscloud.cn/) on August 2, 2021, were used as the original data. The average temperature on that day was 26.2℃, with no rainfall and the wind was less than 3 levels. The cloud cover within the remote sensing image was 5.38%. Overall, the satellite imaging quality on that day was good, with clear landforms and minimal cloud and striping in the study area, making it suitable for research purposes.

Land surface temperature retrieval

The surface temperature refers to the temperature detected by satellite sensors that reflects the intensity of thermal radiation emitted from the ground. According to previous studies, two thermal infrared bands (Band 10 and Band 11) in Landsat 8 TIRS can be used to retrieve land surface temperature (Mashu and Puzhi 2020). However, due to unstable parameters of Band 11, the US Geological Survey (USGS) recommends using Band 10 to retrieve land surface temperature instead of using the segmentation window algorithm that applies both Band 10 and Band 11 (Malakar et al. 2018). When the atmospheric water vapor content (PWV) is less than 3g·cm^{-2}, a single-channel algorithm is an effective method for retrieving land surface temperature. However, due to high atmospheric water vapor content in Xi'an during the summer, using a single-channel algorithm may not yield accurate results. Therefore, this study uses atmospheric correction (radiative transfer equation method) to retrieve land surface temperature. The basic principle of this method is to first estimate the influence of the atmosphere on the surface thermal radiation, and then subtract this part of the atmospheric influence from the total thermal radiation observed by the satellite sensor, to obtain the surface thermal radiation intensity. Then, the thermal radiation intensity is converted into the corresponding land surface temperature (Wang et al. 2019). In practical operations, the specific steps include image radiometric calibration, calculation of vegetation coverage, surface emissivity, black body radiance, and surface temperature. The entire process involves data processing using the Environment for Visualizing Images (ENVI). Primarily, the calculation of L_λ is performed using the atmospheric correction formula as shown in eq. (1).

$$L_\lambda = [\varepsilon B(T_S) + (1-\varepsilon)L\downarrow]\tau + L\uparrow \qquad (1)$$

Where L_λ represents the radiance value of thermal infrared band (band 10); ε represents the surface emissivity; B (TS) represents the blackbody thermal radiance; L↑ represents the upward atmospheric radiance; L↓ represents the downward atmospheric radiance; τ represents the atmospheric transmittance in thermal infrared band. The values of L↑, L↓, and τ can be obtained from the NASA website (http://atmcorr.gsfc.nasa.gov), which are 3.53 W/ (m^2·sr·μm), 5.43 W/

Table 1. Classification of 40 urban parks in Xi'an.

Type of park	Park name
Comprehensive park	Revolution park, New millennium park, Lianhu park, Shaanxi folk-custom showplce, Wenjing park, Textile park, Labor park, Infinity park, Children's park, New century park, Banpo neolithic park
Ecological park	Guangyuntan park, Yanming lake park, Taohuatan, Tang paradise, Yunshui park, Qujiang ruins park, Xi'an international golf club, Weiyang lake park, Xi'an expo park, Xingqing palace park
Theme park	Daminggong relic park, Xi'an martyrs cemetery, Changle park, Wenjingshan park, Yongyang park, Duyi ruins park, Sports park, Muta temple site park, Xi'an botanical garden, Hongguang park, Site of epang palace, Shaanxi hotel, Yannan park, Fengqing park, Shanglin yuan no.4 site park, Black dragon temple
Belt park	Hancheng lake park, Tang city wall ruins park, West side ring city park

(m^2·sr·μm), and 0.57, respectively. The calculation of surface emissivity ε adopts weighted mixing model based on land cover types (Chatterjee, Singh et al. 2017), which is expressed as eq. (2) and eq. (3):

$$\varepsilon = 0.004P_V + 0.986 \quad (2)$$

$$P_V = (NDVI - NDVI_{soil})/(NDVI_{veg} - NDVI_{soil}) \quad (3)$$

In the formula, P_V represents vegetation coverage; NDVI represents normalized difference vegetation index; $NDVI_{soil}$ and $NDVI_{veg}$ respectively represent the NDVI values of areas with bare soil or no vegetation coverage and areas completely covered by vegetation (NDVI values of pure vegetation pixels). Typically, $NDVI_{soil}$ is set to 0.05 and $NDVI_{veg}$ is set to an empirical value of 0.70. Then, the calculation of B (T_S) is performed based on the Planck's law, as shown in eq. (4):

$$B(T_S) = [L_\lambda - L\uparrow - \tau(1-\varepsilon)L\downarrow]/\tau\varepsilon \quad (4)$$

Finally, the formula for surface temperature inversion result is as shown in eq. (5):

$$T_S = K_2/\ln(K_1/B(T_S) + 1) \quad (5)$$

Where, for Landsat8 TIRS band 10, K_1=774.89 W/ (m^2·sr·μm), K_2=1321.08 K.

Park feature parameter extraction

To comprehensively evaluate the influencing factors of the urban park's heat island effect, based on the basic characteristics of the park, they can be divided into two categories: park landscape composition and park landscape configuration. Previous studies have shown that these factors have a significant impact on the park's heat island effect, ensuring that the selected variables are relevant and can accurately analyze this relationship. However, the specific relationship between related indicators and the urban park cool island effect still requires further exploration. There is limited research on the relationship between the park cool island effect indicators used in this study (LPCI, PCE, PCI, PCG). Therefore, we use 5 widely used park landscape composition indicators and 3 park landscape configuration indicators (Table 2) to describe the park's attribute features. The selection criteria for these indicators are as follows: (1) based on previous research; (2) convenient for calculation and understanding; (3) accurate in describing the park; (4) possessing practical significance.

Quantitative the cooling effect

Cooling model construction

Previous studies have shown that the cooling range of urban parks is approximately 1-2 times their own size, and the urban heat island effect usually occurs within a range of 500m (Toparlar, Blocken et al. 2018). Therefore, this study created a buffer zone within 500m of the park boundary and divided it into 20 buffer rings with a width of 25m, as shown in Fig. 3. To analyze the cooling effect of the urban park's heat island effect on the average surface temperature of urban construction land within the buffer zone, this study established a surface temperature-distance function relationship with the distance from the park boundary to the buffer zone as the independent variable l and the average surface temperature of each buffer ring as the dependent variable T. The fitting curve results showed that a third-degree polynomial function T (l) could best describe this relationship, and the model can be expressed as shown in eq. (6):

$$T(l) = al^3 + bl^2 + cl + d \quad (6)$$

where a, b, c, and d represent the fitting coefficients of the third-degree term, second-degree term, first-degree term, and constant term in the polynomial function, respectively.

Cold Island indicator definition

As shown in Fig. 4, with the increase in distance from the park boundary, the surface temperature of the buffer zone gradually increases, but the rate of temperature growth gradually decreases until it reaches 0. At this point, the first derivative of the function T (l), denoted as T' (l), equals 0, and the buffer zone reaches its maximum surface temperature, defined as the first

Table 2. Landscape indicators used in the study.

Index and Abbreviation	Calculation	Description
Landscape composition		
Park area, PA	PA = area of park	Measure the area of the park
Park perimeter, PP	PP = perimeter of park	Measure the perimeter of the park
Water area, WA	WA = area of park water	Measure the area of the park water
Green area, GA	GA = area of green space	Measure the area of the green space
Impermeable surface area, ISA	ISA = area of impermeable surface	Measure the area of the impermeable surface
Landscape configuration		
Park shape index, PSI	PSI = 0.25PP/$\sqrt{PA}$	Use area and perimeter to describe the complexity of the park shape
Patch density, PD	PD = n/A×10000, A = area of land cover, n = the number of patches in a park	Describe landscape porosity and reveal the degree of landscape fragmentation
Edge density, ED	ED = $\sum_{i=1}^{m} Ei$ / A×10000, E*i* = perimeter of patch *i*	The length of edges between patches of heterogeneous landscape elements

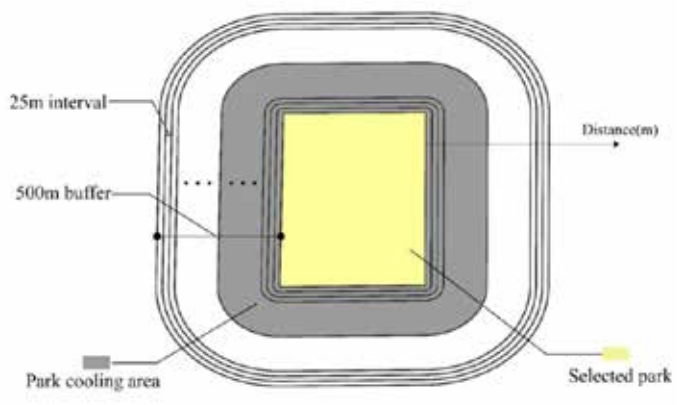

Fig. 3. Schematic diagram of buffer zone establishment.

inflection point. It determines the distance at which the surface temperature of the buffer zone first decreases with increasing distance from the park (Huang et al. 2018). When there is no inflection point in the T (l) function, the inflection point is represented by the minimum value of the first derivative of T (l). Beyond this inflection point, the park no longer has a significant urban heat island effect. The surface temperature at the inflection point is defined as the surface temperature T_L of the park surroundings, and the distance from the park boundary to the first inflection point is defined as L. The cold island index defined in this study is as follows:

(1) The maximum cold island intensity (LPCI) is defined as the difference between the surface temperature T_L of the first inflection point and the average surface temperature T_{park} inside the park, as shown in eq. (7). LPCI is used to measure the temperature difference between the surface of the park and the surrounding environment.

$$LPCI = T_L - T_{park} \qquad (7)$$

(2) Park Cold Island Efficiency (PCE) is defined as the product of the maximum cold island intensity (LPCI) and cold island area (PCA) of a park, divided by the park area (PA), as shown in eq. (8). It measures the cold island effect produced by a park per unit area, essentially reflecting the input-output ratio from an economic perspective. As PCE increases, the actual benefits associated with the cold island effect of a park also increase.

$$PCE = \frac{LPCI \times PCA}{PA} \qquad (8)$$

However, the cold island effect of a park has a nonlinear relationship with distance, and the maximum value indicator cannot reflect the spatial continuity of the cold island effect. The strength of the cold island effect of a park cannot be evaluated solely from a maximum value perspective but should also be evaluated from an accumulation perspective. Therefore, two accumulation indicators, park cold island intensity and park cold island gradient, are defined to continuously describe the cold island effect of urban parks.

(3) Park Cold Island Intensity (PCI) is defined as the ratio of the reduction in surface temperature at the maximum cooling distance (first inflection point) to the total surface temperature, as shown in eq. (9). It reflects the degree of cooling felt by residents, and as PCI increases, the degree of surface temperature reduction felt by local residents also increases.

$$PCI = \frac{L \times T_L - \int_0^L T(l)dl}{L \times T_L} \qquad (9)$$

Where L represents the maximum cold island distance of a park, and T_L represents the surface temperature at the maximum cold island distance. Since the cold island effect of a park is a continuous process in space, $L \times T_L$ represents the cumulative temperature of all continuous spatial points without interference from the cold island effect of a park. The T (l) function represents the actual curve of surface temperature change in the surrounding environment when a cold island effect is present and exerted by an urban park. $\int_0^L T(l)dl$ represents the actual cumulative surface temperature from the boundary of the urban park to the maximum cold island distance, and $L \times T_L - \int_0^L T(l)dl$ represents the cumulative cooling temperature of the park (which does not actually exist). Therefore, PCI refers to the ratio of the cumulative reduction in surface temperature to the total surface temperature.

(4) Park Cold Island Gradient (PCG) is defined as the ratio of the reduction in surface temperature to the cold island distance of a park, as shown in eq. (10). It represents the cumulative cooling amount of a park at each cold island distance, that is, the degree of cooling. PCG reflects the heat absorption rate of the cold island process of a park. The higher the PCG, the higher the heat absorption rate, and vice versa.

$$PCG = \frac{L \times T_L - \int_0^L T(l)dl}{L} \qquad (10)$$

Data Analysis

Firstly, to analyze the spatial heterogeneity of surface temperature in urban parks, this study uses the hot spot analysis tool in spatial clustering analysis to calculate Getis-Ord Gi* statistics for each feature in the data, in order to identify the clustering of high or low surface temperature values in the study area. ArcGIS 10.8 software is used for the hot spot analysis of surface temperature spatial heterogeneity. Secondly, using the

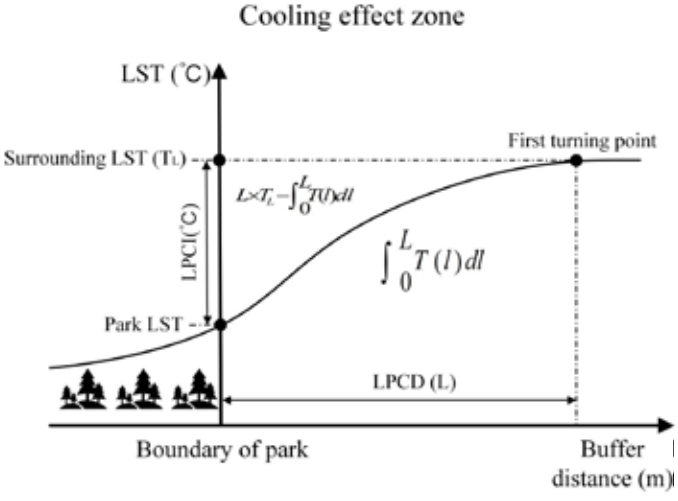

Fig. 4. Surface temperature variation curve during cold island process in park.

distance from the park boundary as the independent variable and surface temperature as the dependent variable, a cubic function model is fitted to examine the cooling effect of urban parks on the surrounding area. The fitting results can demonstrate the accuracy of the results to some extent, as indicated by the R^2 value. Next, Pearson correlation coefficients are used to analyze the correlation between various heat island indicators and park characteristic parameters. The values of Pearson correlation coefficient range from -1 to 1, and the significance level (p-value) determines the degree of correlation. Generally, differences with $p<0.05$ are considered statistically significant. SPSS 26.0 software is used for Pearson correlation analysis of heat island indicators and their influencing factors. Finally, the standard deviation ellipse tool is used to analyze the clustering distribution of cold spot temperatures inside and outside the park. The standard deviation ellipse is a tool that can simultaneously analyze the direction and distribution of points. The major axis of the ellipse represents the direction of the park's cold island propagation. A larger ellipticity indicates a more significant directionality of the data.

Results

Spatial distribution characteristics of urban thermal environment

As shown in Fig. 5a, according to the inversion results of surface temperature, the maximum surface temperature in the main urban area of Xi'an on August 2, 2021, was 52.46°C, the minimum was 25.30°C, and the average surface temperature was 38.26°C. From the spatial pattern of surface temperature distribution, the urban heat island effect in the main urban area of Xi'an is obvious, especially in densely populated areas such as large public places, residential areas, commercial areas, and industrial areas. The surface temperature shows a general trend of "high in the middle and low on the four sides" and "high in the southwest and low in the northeast", with high temperature areas concentrated in the city center and the west. Of course, there are also many areas with lower temperatures in the city, which are concentrated in urban parks and river and lake landscapes with higher blue-green coverage, corresponding to urban ecological infrastructure, and their low temperature plays a cooling island effect in the city. Observing the spatial distribution of surface temperature in the park area marked by the green line in Fig. 5a, the spatial distribution of surface temperature in each park with ring-shaped low temperature distribution to varying degrees was analyzed, indicating that there are urban heat island effect holes in each park. To further understand the spatial heterogeneity of surface temperature in the main urban area of Xi'an, this study conducted cold-hot spot analysis (Getis-Ord Gi*) to explore the spatial clustering characteristics of high and low surface temperatures within the main urban area. (Fig. 5b). The cold spot area corresponds to the coverage area of vegetation and rivers, while the hot spot area corresponds to the coverage area of impermeable surface, which is consistent with the analysis results of surface temperature. Regarding the park areas, the results of cold-hot spot analysis show that there is a 65.43% overlap between park area and cold spot area (areas with cold spot confidence exceeding 90%), indicating that urban parks have a significant cooling island effect.

Urban park cold island effect

Quantification results of park cold island

To further quantify the cooling effect of parks, this study established a surface temperature-distance function fitting curve, as shown in Fig. 6. The results showed that the fitting curves of different parks had a high degree of similarity and presented an overall trend of increasing and then remaining unchanged. This indicates that parks have a significant cooling effect on a certain area around them, but the cooling effect weakens with increasing distance. Temperature data from 40 parks in the city's built-up areas were extracted, and the average surface temperature inside the park was compared with the average surface temperature of the surrounding environment (surface temperature TL at the maximum cold island distance), as shown in Fig. 7. The average surface temperature inside the park was 2.24°C lower than that of the surrounding environment, and 0.82°C lower than the average

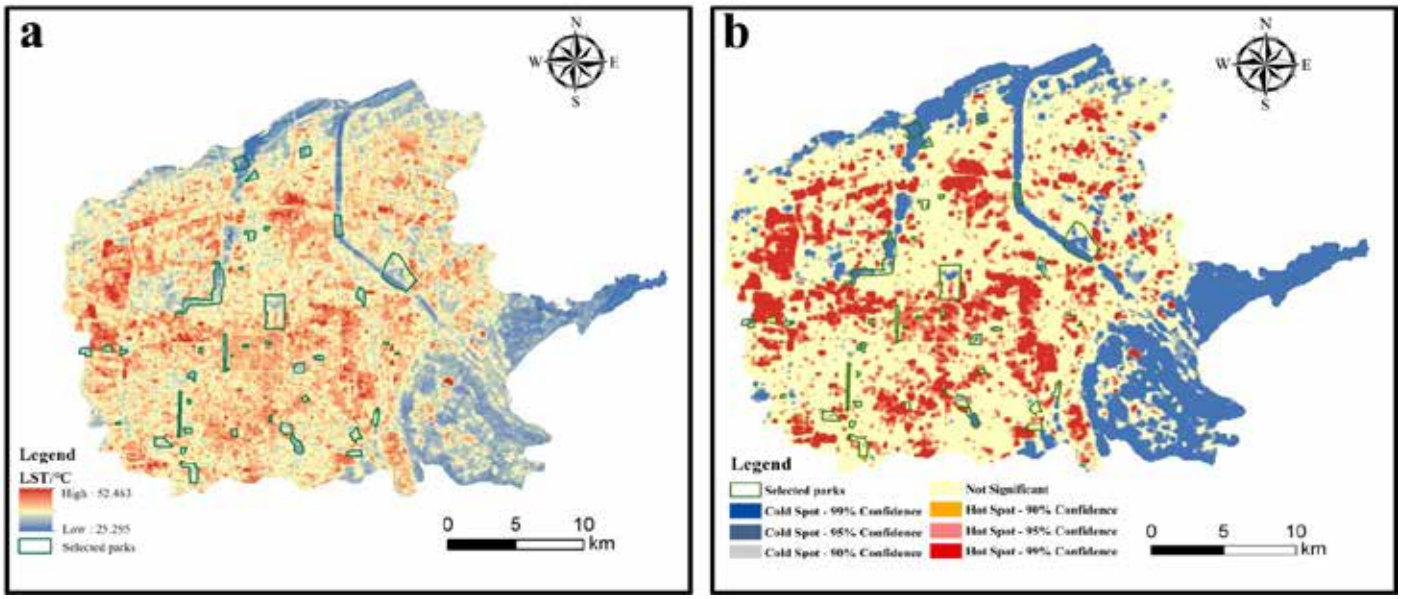

Fig. 5. Spatial patterns of (a) LST and (b) cold-hot spot area distribution.

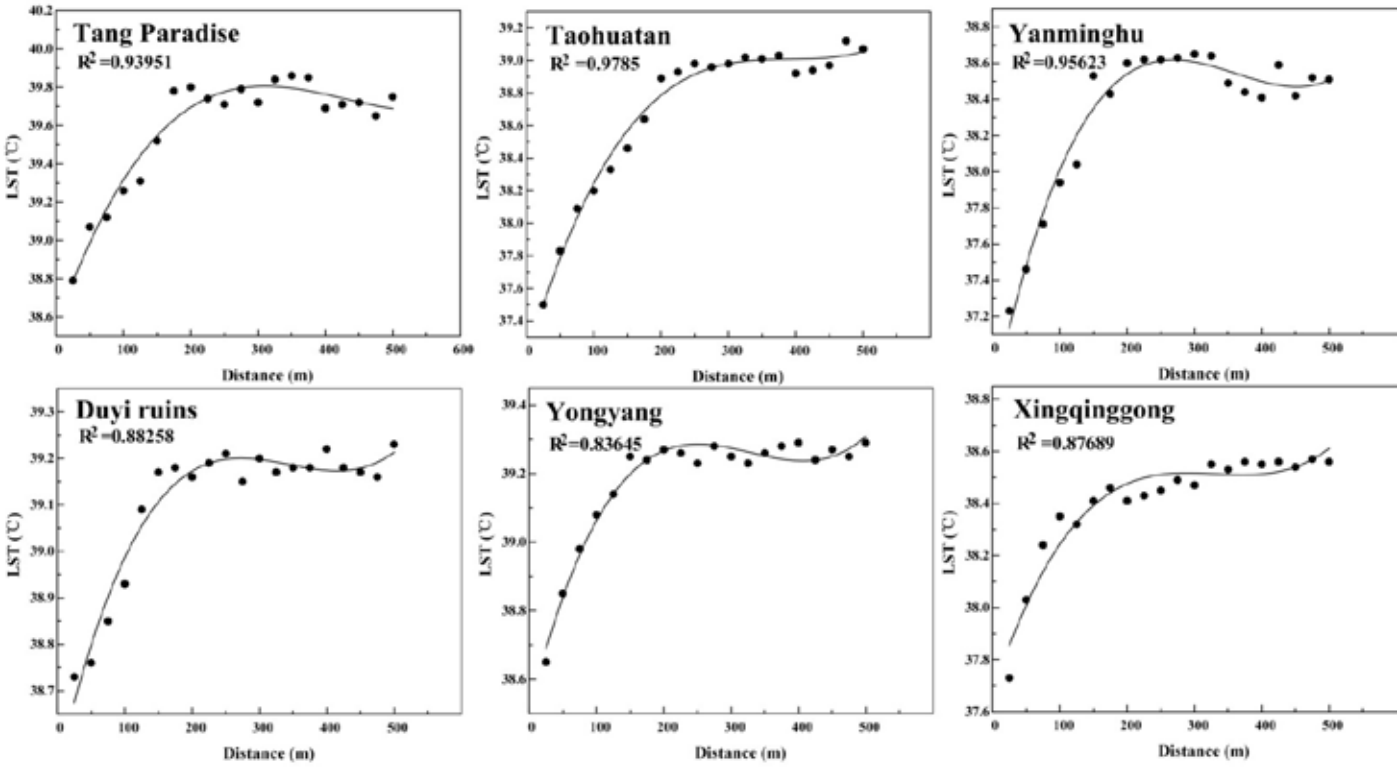

Fig. 6. Surface temperature-distance fitting curve of some parks.

temperature in the main urban area of Xi'an, which also confirms the significant cooling effect of urban parks on the surrounding environment.

Based on the park's cooling model, the calculation results of the four cold island effect indicators (LPCI, PCE, PCI, PCG) for 40 urban parks in the city's built-up areas are shown in Fig. 8. These results exhibit varying degrees of fluctuations among the indicators across the 40 parks. The LPCI of parks ranged from 0.35 to 4.44℃, with an average of 2.22℃ (Fig. 8a); the PCE of parks ranged from 1.1 to 22.45, with an average of 8.16 (Fig. 8b); the PCI of parks ranged from 0.0001 to 0.0223, with an average of 0.0074 (Fig. 8c); and the PCG of parks ranged from 0.0033 to 0.7875℃, with an average of 0.2918℃ (Fig. 8d). Overall, most of the parks had cold island effect indicators that were not significantly different from the average, but there were also some parks with cold island effect indicators that were far above the average, such as the LPCI of Park 23 and the PCE of Parks 4, 27, and 36. Park 30 had significantly lower values for all indicators, mainly due to the huge differences in park area (1.5-346.4ha).

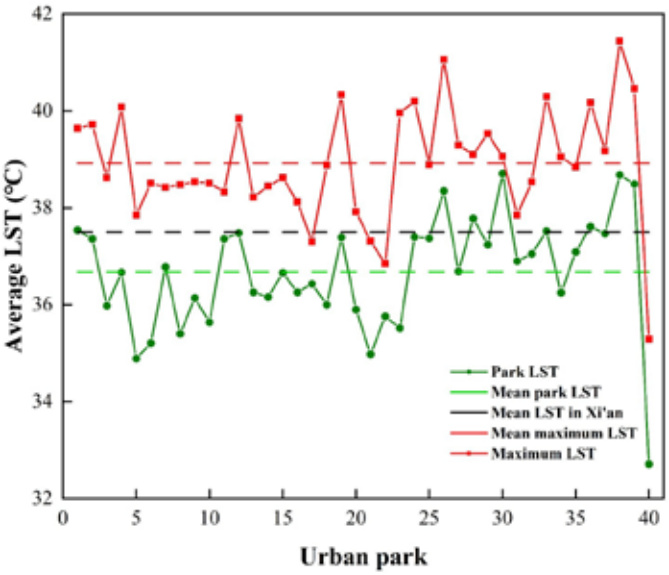

Fig. 7. LST of 40 parks in built-up areas and surrounding environments.

Analysis of influencing factors of cold island in parks

This article uses Pearson correlation coefficient to measure the correlation between the urban park's cold island effect indicators (LPCI, PCE, PCI, PCG) and various influencing factors (such as park area and perimeter, area of various landscape compositions, PSI, PD, ED), as shown in Table 3. Many studies have shown that the park's area and perimeter have the most significant impact on LPCI. In this study, LPCI showed a significant positive correlation with the park area and green area, which increased with the increase of its indicators. Among them, the park area had the highest correlation ($r=0.568$, $p<0.01$). However, when the park area reached a certain threshold, the growth rate of LPCI significantly slowed down, as shown in Fig. 9a, and the slope of the function fitting curve decreased significantly when the park area reached 20 hectares. It is worth noting that the threshold is not fixed and is also affected by the geographic location and climate of the park.

PCE showed a negative correlation with the park area, perimeter, and other landscape compositions, indicating that the input-output ratio of its cooling effect decreases as these park parameters increase. However, PCE showed a high positive correlation with the park patch density (Fig. 9b) ($r=0.631$, $p<0.01$). As the park patch density increases, the landscape fragmentation increases, the landscape diversity increases, and the park's cooling efficiency also increases.

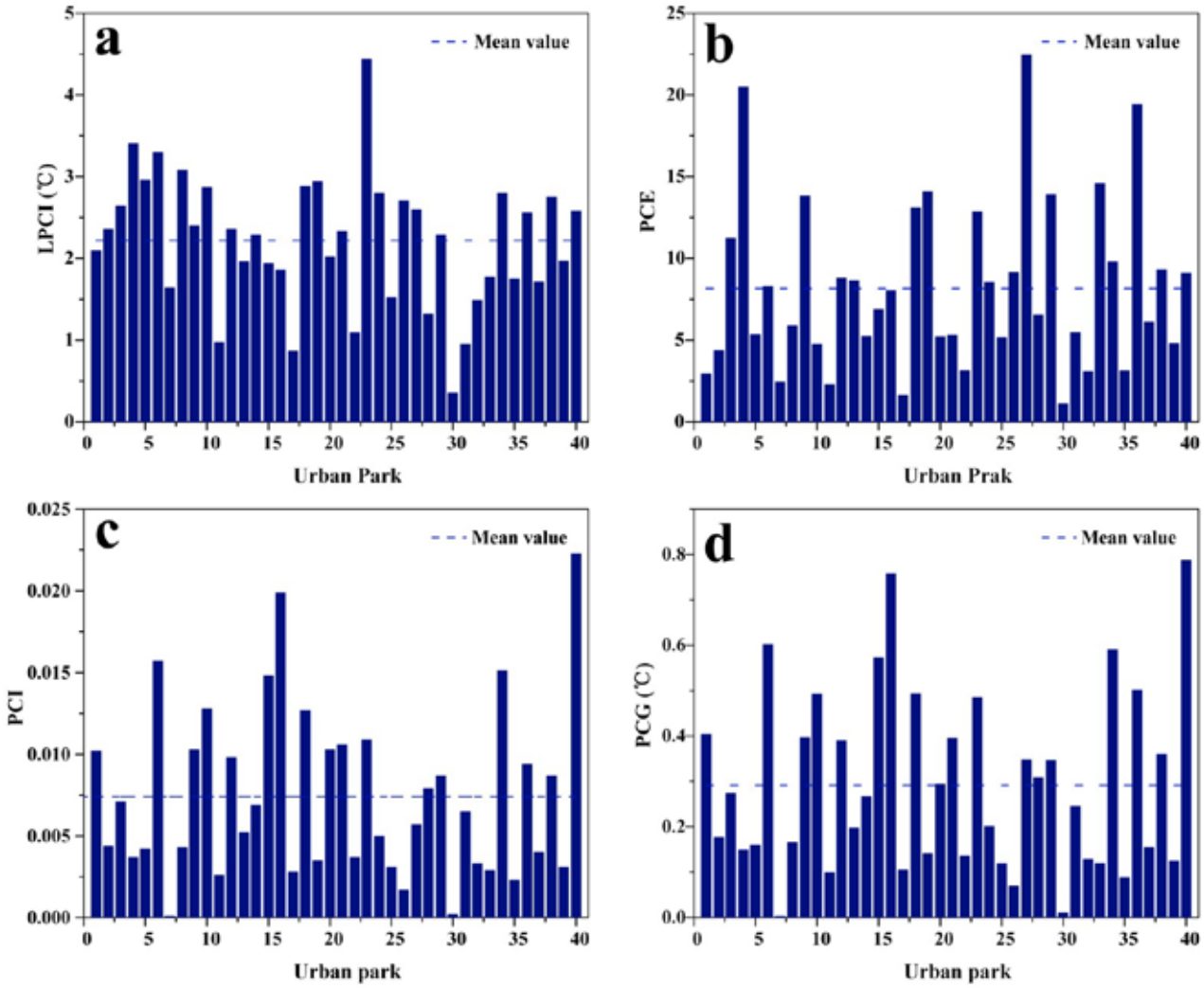

Fig. 8. Cold island effect indicators of 40 urban parks.

As shown in Fig. 9c, PCI showed a high positive correlation with the park green area (r=0.471, p<0.05). Because the park green area has a higher vegetation coverage and higher heat exchange efficiency with the surrounding environment, the proportion of the reduced surface temperature to the total temperature of the surrounding environment is larger, and the cooling process is more intensive, resulting in a higher PCI.

PCG showed a high positive correlation with the park perimeter, as presented in Fig. 9d (r=0.359, p<0.05) and the park shape index (r=0.298, p<0.05). According to the definition of the park shape index, as the park area remains constant, the park shape index increases with the increase of the park perimeter, and the park boundary shape becomes more complex. Parks with large perimeters and complex boundary shapes can have

Table 3. Correlation coefficient between the cold island index and the influencing factors of Xi'an Park.

Characteristics	LPCI	PCE	PCI	PCG
Area	0.568**	-0.362*	0.336*	0.321*
Perimeter	0.485**	-0.337*	0.381*	0.359*
Water area	0.414**	-0.343*	0.297	0.276
Green area	0.566**	-0.332*	0.471*	0.316*
Impermeable surface area	-0.521**	-0.38*	-0.145	-0.149
Park shape index	0.505**	-0.271	0.417*	0.298*
Patch density	0.048	0.631**	0.103	0.068
Edge density	0.154	0.537**	-0.119	-0.158

* Represent the significance at 0.05 level, respectively.
** Represent the significance at 0.01 level, respectively.

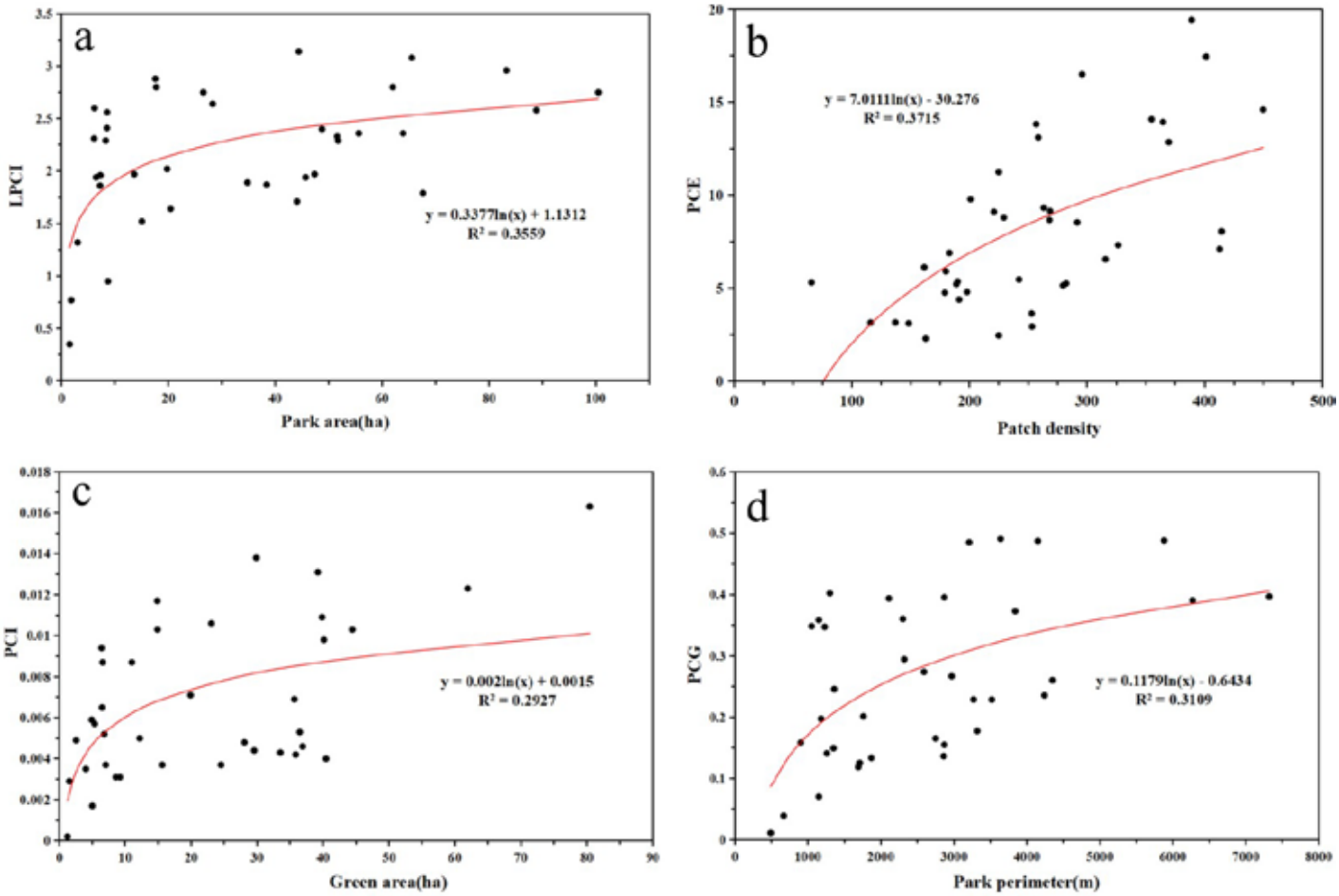

Fig. 9. The fitting curve of each cold island effect index and its maximum influencing factor.

a stronger connection with the surrounding environment and produce greater cooling effects. Therefore, urban parks with more fragmented boundaries are more conducive to reducing the temperature of the surrounding environment.

The non-permeable surface area showed a negative correlation with all cold island effect indicators, as the non-permeable surface has poor water permeability, reduced subsurface infiltration, lower heat capacity, and faster heat absorption and release. Therefore, an increase in the non-permeable surface area in the park severely reduces its cooling effect. In addition, Xi'an is located deep inland, and water resources are relatively scarce. The water area in the park is relatively small, so the correlation between the water area and the various cold island indicators in the park is not high.

Analysis of cold island characteristics of different types of parks

The cold island indicators of various parks were normalized, and the characteristics and influencing factors of the cold island indicators of four types of urban parks were further compared and analyzed (Fig. 10). The results showed that the four cold island indicators of theme parks were not high because they have distinct individual characteristics, mainly focusing on cultural tourism or amusement, such as heritage parks and amusement parks. They provide cultural services for specific citizens, and the proportion of impervious surfaces such as buildings and roads in the parks is relatively high, while the proportion of green spaces and water bodies is relatively low. Moreover, the parks are generally not large, with an average area of 35.74 ha, so the cooling effect is not obvious. The PCE of ecological parks is relatively low, while LPCI, PCG, and PCI are generally large. These parks usually have a larger area, with an average of 58.51 ha. The larger park area will inevitably lead to a generally lower PCE. Most ecological parks are located on the outskirts of the city, focusing on ecological benefits, playing a role in wind and sand control and water conservation. The water and green coverage inside the park is high, and it is scientifically configured, so the cooling range of ecological parks is large, and the cooling effect is significant. The PCE and LPCI of comprehensive parks are relatively large, while PCI and PCG are relatively small. These parks are usually located in the busy areas of the city, with complex land use conditions, resulting in a small park area, with an average of about 6.02 ha, and a large shape index. The park boundary shape is irregular, the internal patch density is high, and the landscape is fragmented. Therefore, it can be seen from the input-output ratio of the park's cold island that the cooling range of the park is significantly larger than the park area, indicating that the park's cold island efficiency is high and economically efficient. The four cold island indicators of strip parks are relatively high. These parks are widely distributed throughout the city, such as on both sides of roads and along rivers. They have a narrow shape and limited blue-green space layout.

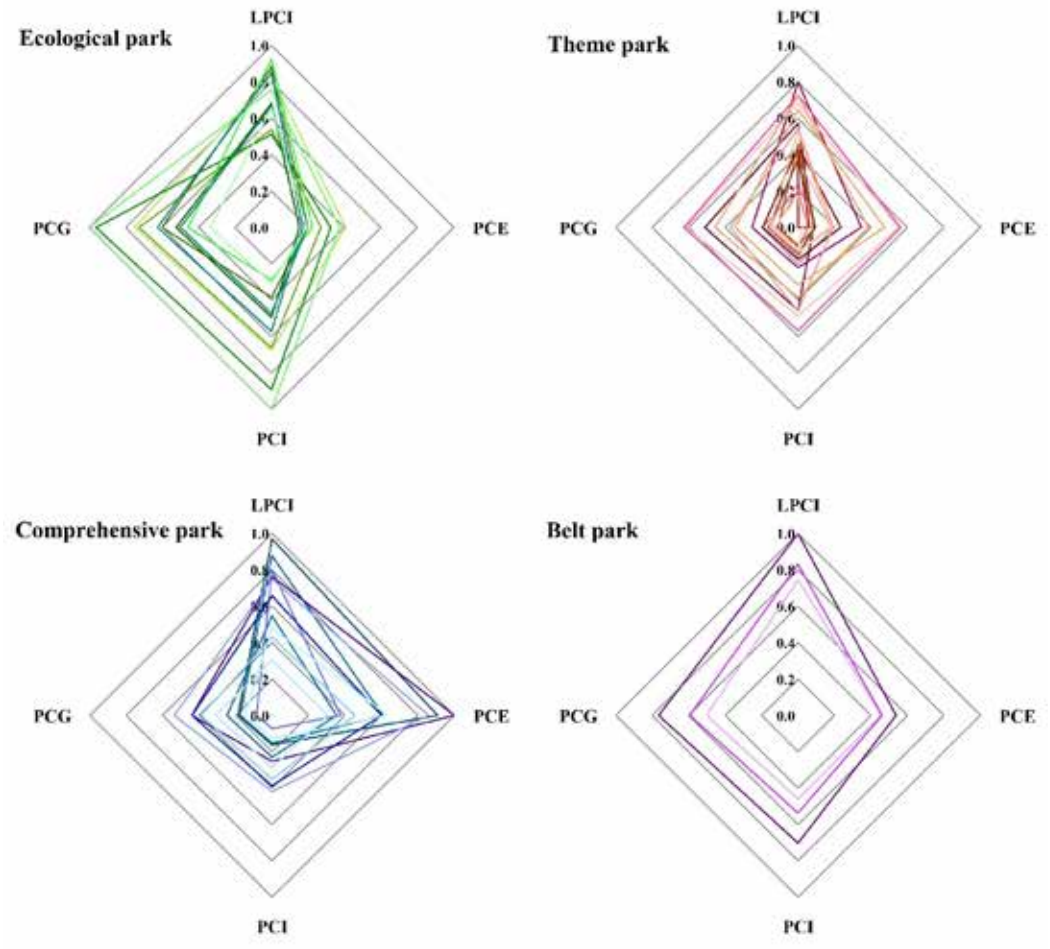

Fig. 10. Cold island effect indicators of four park types.

However, compared with parks of the same area, this type of park has more open boundaries, which can penetrate with the surrounding environment and improve heat exchange capacity. Therefore, the cooling effect is very significant.

In summary, urban parks classified based on different social service types will produce different cooling effects, and parks of the same type will also produce different cooling effects due to factors such as park area and shape index. Therefore, through multi-angle and multi-faceted integrated analysis of urban parks, the stable balance point between urban ecological environment and human activities can be promoted.

Directional analysis of park cold island

Different social uses and locations of parks can lead to significant differences in park land use and changes in underlying surface characteristics due to variations in internal building, vegetation, and water body configurations. Therefore, hotspot analysis and standard deviation ellipse tools can be used to analyze the directional spread of the urban heat island effect for different types of parks (Fig. 11). Hotspot analysis is used to obtain maps of statistically significant hotspots (high values) and cold spots (low values) of surface temperature by performing Getis-Ord Gi* statistics for each element in the temperature data. Standard deviation ellipse is a tool that can analyze the direction and distribution of points simultaneously. In this study, only cold spots were chosen as the research object by removing the hotspots obtained from hotspot analysis. The greater the ratio of the ellipticity of the obtained ellipse, the more significant the directional tendency of the data.

The results showed that for ecological parks, taking Xingqing Palace Park as an example (Fig. 11a), the cold spots were concentrated in the green areas and water bodies within the park. Due to the high proportion of water bodies in the park, the direction of the cold island was generally consistent with the flow of water bodies and showed a southwest-northeast direction. There was no significant bias in the direction of the cold island outside the park. For comprehensive parks, taking Revolution Park as an example (Fig. 11b), due to the small park area, cold spots were dist ributed throughout the park. Influenced by the park's shape, the internal cold island spread northwest-southeast, but there was no significant directional tendency outside the park. For theme parks, taking Xi'an Botanical Garden as an example (Fig. 11c), the cold spots were concentrated in the green areas due to the dense vegetation and extremely low proportion of water bodies within the park. The internal cold island showed a north-south direction consistent with the direction of the green areas. With extensive green areas distributed around the park, the external cold island spread in a northwest-southeast direction. For strip parks, taking Hancheng Lake Park as an example (Fig. 11d), the cold spots along the boundary of the park showed a strip distribution influenced by the park's shape. The cold island of the park spread in a southwest-northeast direction with significant directional tendency, consistent with the direction of cooling inside the park.

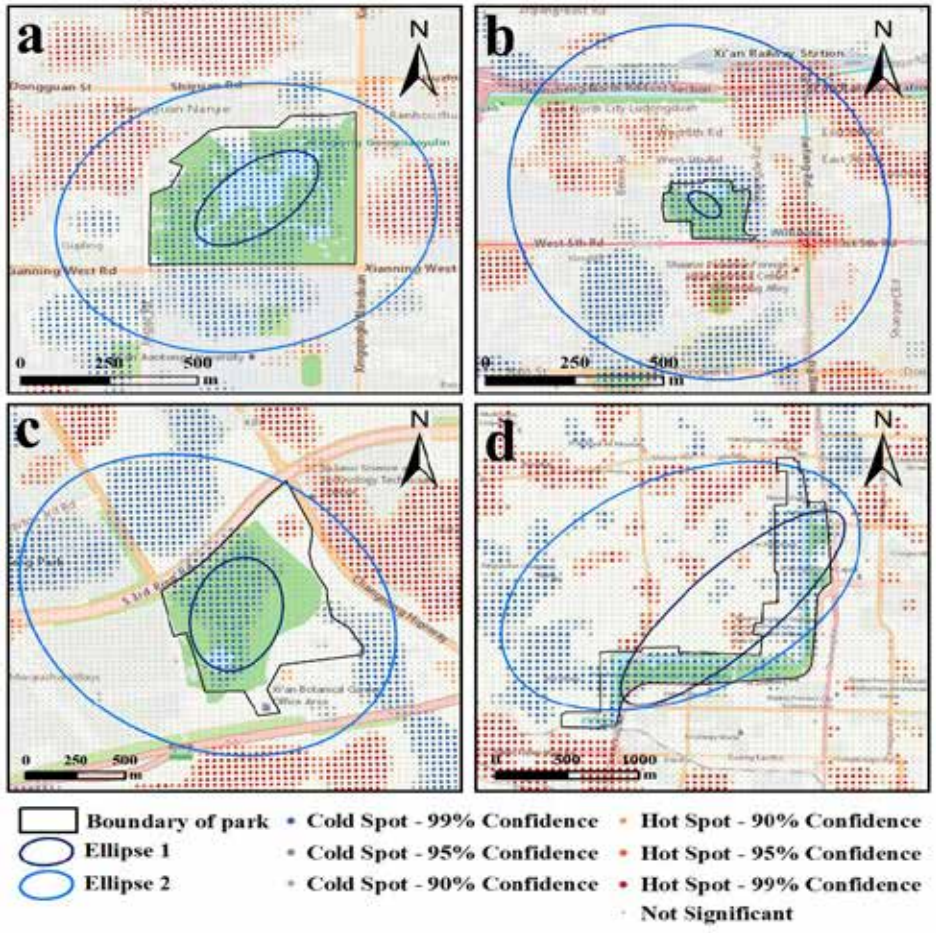

Fig. 11. Directionality of cold island in built-up area park: (a) Xingqing Palace Park; (b) Revolution Park; (c) Xi'an Botanical Garden; (d) Hancheng Lake Park.

In summary, the directional tendency of the urban heat island effect in parks is not closely related to the type of park. However, for the directional tendency of the internal cold island effect in parks, the park's shape has the greatest influence, followed by the influence of water bodies. For the surrounding area of the park, the widespread distribution of buildings and hard-surfaced roads greatly hinder the diffusion of the cold island effect in the park, while the green areas covering the surrounding area provide a good cooling foundation, determining the direction of external cold island spread.

Discussion

The impact of urban parks on surface temperature

The research results indicate that the average surface temperature in urban parks in the main urban area of Xi'an is significantly lower than the average surface temperature in the surrounding environment without the cooling effect of parks, demonstrating the ability of urban parks to alleviate urban heat. This is consistent with previous research findings(Chen et al. 2021, Liao et al. 2023). Among the 40 urban parks in the study area, Hancheng Lake Park has the largest ΔLST (temperature difference between park and surroundings), with a park area of 320 hectares and a coverage of greenery and water bodies reaching 87.87%. Its irregular belt-shaped boundary, combined with various factors, contributes to the park's strong cooling capability. Furthermore, the Landsat 8 satellite images used to retrieve surface temperatures were not captured at the hottest time of the day. When the temperature is at its highest, the corresponding ΔLST will be even greater.

Meanwhile, the distribution and cooling effect of urban parks in Xi'an are closely related to the level of urban development. The central area of the old city, represented by Yanta District, has significantly higher temperatures compared to other areas. This can be attributed to the large population flow, traffic congestion, and dense buildings in the main urban area, which collectively cause heat concentration and increased urban air temperature. Additionally, the scarcity of housing in the old city forces priority on the construction of residential buildings over ecological facilities during urban renewal, further exacerbating the scale of the UHI effect. On the contrary, the low-temperature area is in the northern part of the city, corresponding to Weiyang District. This area has well-developed ecological engineering and numerous large urban parks that regulate the local climate, effectively limiting the occurrence of the UHI effect. Therefore, to alleviate the urban heat environment problem, it is necessary to consider improving the current urban planning schemes and prioritize the construction of comprehensive ecological infrastructure. This includes increasing the proportion of urban parks in the old city area to alleviate the high temperatures in the central area. During urban renewal, it is important to consider the dispersed construction of urban parks to increase the proportion of such spaces in high-temperature areas.

In conclusion, urban parks can effectively regulate urban surface temperatures. In the current global context of increasing population, the pressure on urban land resources for providing housing and ecological services is further intensified. Therefore, in the process of urban spatial management, it is imperative to design urban parks in a reasonable manner based on established thresholds and demands to optimize their cooling effects.

Planning and design plan for urban parks

Urban parks are planned and designed public space areas used for multiple social purposes. They serve as recreational areas for urban residents, play an important role in the urban blue-green landscape, and maintain the ecological environment of the city, especially in reducing the negative impact of the urban heat island effect. Although previous studies have considered the correlation between park attributes and park cooling effects as an important indicator of planning and design, they have not explored cooling effects from multiple angles (Xiao et al. 2018). For example, the maximum cool island distance of a park increases as the park area increases. Although this study validates this effect, it also found that the maximum cool island distance does not increase linearly with park area. It is unreasonable to significantly increase park area to enhance cooling effects. Therefore, it is not appropriate to measure park cooling effects from a single angle.

Various urban parks have different functions, and it is crucial to plan and design urban parks according to different geographical features and construction needs (Mandeli 2019). To maximize the benefits of urban parks within investment constraints, designers should consider different cooling effects based on their primary goals. In this regard, the difficulty in designing urban parks is not simply optimizing a single cool island index, but how to maximize a specific cool island index without reducing other cool island indices.

In this study, four cool island indices were used to measure the cooling effects of parks from the perspectives of maximum value and accumulation, each index being influenced by different factors. Therefore, in the process of designing and planning urban parks, appropriate choices should be made based on construction needs. For example, if a park is intended to have a strong personality and benefits are the primary goal, with cooling as a secondary consideration, it can be designed as a theme park, which has a low cooling effect. If a park aims to benefit more residents, it should be designed as an ecological park, which has a large PCI and PCG and a wide cooling range. If the park's planning land is scarce, and construction costs are limited, a comprehensive park is a good choice, which has a high PCE and good economic efficiency. If an ecological corridor is needed to guide residents' exercise, a strip park can be designed, which has good ecological benefits and strong spatial guidance. After clarifying the cooling effect, it is necessary to consider the landscape pattern and spatial form comprehensively to meet the various needs of urban residents and improve their quality of life through providing urban blue-green landscape.

Limitations and outlook of the study

This study evaluates the urban park cool island effect based on remote sensing images and considers the maximum impact index and spatial continuity accumulation index as evaluation standards. The research results can provide theoretical basis for future alleviation of urban heat environment and urban park planning and design. However, this study has certain limitations. Firstly, there may be errors in the inversion results of surface temperature. Due to the limitations of current technology, the spatial resolution of Landsat8 satellite in obtaining remote sensing images is limited (the spatial resolution of TIRS sensor used in this paper is 100 meters). This low spatial resolution has a significant impact on the results, and future use of higher resolution Landsat series data can improve the reliability of the research. Secondly, the cooling effect of the park studied in this paper is concentrated on a single day in a single season (summer), which may be accidental. In the future, different seasons and dates can be explored to make the research results more comprehensive. Thirdly, the impact of park water bodies on the cooling effect can be studied in the future, as water bodies with the highest specific heat capacity have a more significant cooling effect on cities. Fourthly, different climates and geographical locations will have an impact on the research results (Saaroni et al. 2018).

This paper focuses on Xi'an city as the research object, and in the future, urban areas in different geographical regions can be compared at the same time for research. External environmental factors of parks, such as building types and human activities, may affect the cooling effect of parks, and appropriate research can be conducted in the future.

Conclusions

This study focuses on 40 urban parks in the main urban area of Xi'an city, measuring the cooling effect of the parks from two perspectives: maximum value and cumulative effect. The study enhances the understanding of the cooling degree and spatial continuity of the parks. The results show that urban parks have a significant cooling effect on the surrounding environment, with an average temperature reduction of 2.24℃ within their cold island range. The park area, perimeter, green area, and patch density are significantly correlated with the maximum cooling island intensity and cooling island efficiency. The park perimeter, green area, and park shape index are significantly correlated with the cooling island intensity and gradient. The non-permeable surface is negatively correlated with all cooling island indicators to varying degrees. When the park area reaches the threshold of 20 hectares, the cooling island effect is optimal. Irregularly shaped and highly vegetated parks can achieve better cooling effects. The cooling effect of different types of social service parks varies significantly. Theme parks have lower cooling island indicators and poor cooling effects, while ecological parks have higher cooling island gradients and intensities and a larger cooling range. Comprehensive parks have higher cooling island efficiency and economic benefits, with better cooling effects. Belt parks have higher cooling island indicators than other parks of the same area, with a significant cooling island direction. The research findings enhance people's understanding of the cooling island effect of parks and provide a theoretical basis for urban managers to deal with future urban heat environment issues, as well as a broader perspective for further exploring how to achieve higher cooling effects in parks.

Data availability

The processed data used in the study are available from the corresponding author by reasonable request.

Funding None.

Compliance with Ethical Standards

Conflict of Interest The authors declare no competing interests.

Informed consent All authors have read and approved the final version of the manuscript.

References

Algretawee, H., Rayburg, S. & Neave, M. (2019). Estimating the effect of park proximity to the central of Melbourne city on Urban Heat Island (UHI) relative to Land Surface Temperature (LST). *Ecological Engineering*, 138, pp. 374-390. DOI:10.1016/j.ecoleng.2019.07.034

Anjos, M. & Lopes, A. (2017). Urban heat island and park Cool island intensities in the coastal city of Aracaju, north-eastern Brazil. *Sustainability*, 9, 8, pp. 1379. DOI:10.3390/su9081379

Chatterjee, R., Singh, N., Thapa, S., Sharma, D. & Kumar, D. (2017). Retrieval of land surface temperature (LST) from Landsat TM6 and TIRS data by single channel radiative transfer algorithm using satellite and ground-based inputs. *International Journal of Applied Earth Observation and Geoinformation*, 58, pp. 264-277. DOI:10.1016/j.jag.2017.02.017

Chen, M., Jia, W., Yan, L., Du, C. & Wang, K. (2022). Quantification and mapping cooling effect and its accessibility of urban parks in an extreme heat event in a megacity. *Journal of Cleaner Production*, 334, pp. 130252. DOI:10.1016/j.jclepro.2021.130252

Gao, M., Chen, F., Shen, H. & Li, H. (2020). A tale of two cities: Different urban heat mitigation efficacy with the same strategies. *Theoretical and Applied Climatology*, 142, pp. 1625-1640. DOI:10.1007/s00704-020-03390-2

Gao, Z., Zaitchik, B.F., Hou, Y. & Chen, W. (2022). Toward park design optimization to mitigate the urban heat Island: Assessment of the cooling effect in five US cities. *Sustainable Cities and Society*, 81, pp. 103870. DOI:10.1016/j.scs.2022.103870

Hong, C., Wang, Y., Gu, Z. & Yu, W. C. (2022). Cool facades to mitigate urban heat island effects. *Indoor and Built Environment*, 31, 10, pp. 2373-2377. DOI:10.1177/1420326x221115369

Huang, M., Cui, P. & He, X. (2018). Study of the cooling effects of urban green space in Harbin in terms of reducing the heat island effect. *Sustainability*, 10, 4, pp. 1101. DOI:10.3390/su10041101

Huang, X. & Wang, Y. (2019). Investigating the effects of 3D urban morphology on the surface urban heat island effect in urban functional zones by using high-resolution remote sensing data: A case study of Wuhan, Central China. *ISPRS Journal of Photogrammetry and Remote Sensing*, 152, pp. 119-131. DOI:10.1016/j.isprsjprs.2019.04.010

Li, H., Zhou, Y., Jia, G., Zhao, K. & Dong, J. (2022). Quantifying the response of surface urban heat island to urbanization using the annual temperature cycle model. *Geoscience Frontiers*, 13, 1, 101141. DOI: 10.1016/j.gsf.2021.101141

Liao, W., Guldmann, J.-M., Hu, L., Cao, Q., Gan, D. & Li, X. (2023). Linking urban park cool island effects to the landscape patterns inside and outside the park: A simultaneous equation modeling approach. *Landscape and Urban Planning*, 232, pp. 104681. DOI:10.1016/j.landurbplan.2022.104681

Malakar, N. K., Hulley, G. C., Hook, S.J., Laraby, K., Cook, M. & Schott, J.R. (2018). An operational land surface temperature product for Landsat thermal data: Methodology and validation. *IEEE Transactions on Geoscience and Remote Sensing*, 56, 10, pp. 5717-5735. DOI:10.1109/tgrs.2018.2824828

Mandeli, K. (2019). Public space and the challenge of urban transformation in cities of emerging economies: Jeddah case study. *Cities*, 95, pp. 102409. DOI:10.1016/j.cities.2019.102409

Mashu & Puzhi (2020). Research on surface temperature inversion algorithm based on Landsat8 data: A case study of Urumqi. *Computer and Digital Engineering*, 48, 10, pp. 2316-2320. DOI:10.1088/1755-1315/450/1/012031

Ozgeldinova, Z., Zhanguzhina, A. & Ulykpanova, M. (2023). Spatial and temporal analysis of landscape dynamics in the Kostanay region under an-thropogenic impacts. *Archives of Environmental Protection*, 49, pp.80-94. DOI:10.24425/aep.2023.148687

Peng, J., Dan, Y., Qiao, R., Liu, Y., Dong, J. & Wu, J. (2021). How to quantify the cooling effect of urban parks? Linking maximum and accumulation perspectives. *Remote Sensing of Environment*, 252, 112135. DOI:10.1016/j.rse.2020.112135

Qian, W. & Li, X. (2023). A cold island connectivity and network perspective to mitigate the urban heat island effect. *Sustainable Cities and Society*, 94, 104525. DOI:10.1016/j.scs.2023.104525

Qiu, J., Li, X. &Qian, W. (2023). Optimizing the spatial pattern of the cold island to mitigate the urban heat island effect. *Ecological Indicators*, 154, pp. 110550. DOI:10.1016/j.ecolind.2023.110550

Ruochen, Y., Jia, X., Dan, Z.& Yang, H. (2022). Measuring the Cooling Benefits of Urban Parks and Climate Adaptation Design Strategies. *Chinese Landscape Architecture*, 6, pp. 121. DOI:10.3390/ani12172251

Saaroni, H., Amorim, J. H., Hiemstra, J.& Pearlmutter, D. (2018). Urban Green Infrastructure as a tool for urban heat mitigation: Survey of research methodologies and findings across different climatic regions. *Urban climate*, 24, pp. 94-110. DOI:10.1016/j.uclim.2018.02.001

Sun, C., Wang, Y. & Zhu, Z. (2023). Urbanization and residents' health: from the perspective of environmental pollution. *Environmental Science and Pollution Research*, 30, 25, pp.1-19. DOI:10.1007/s11356-023-26979-2

Toparlar, Y., Blocken, B., v. Maiheu, B. & Van Heijst, G. (2018). The effect of an urban park on the microclimate in its vicinity: a case study for Antwerp, Belgium. *International Journal of Climatology*, 38, pp. e303-e322. DOI:10.1002/joc.5371

Wang, W., Liu, K., Tang, R. & Wang, S. (2019). Remote sensing image-based analysis of the urban heat island effect in Shenzhen, China. *Physics and Chemistry of the Earth, Parts a/b/c*, 110, pp. 168-175. DOI:10.1016/j.pce.2019.01.002

Wu, C., Li, J., Wang, C., Song, C., Chen, Y., Finka, M. & La Rosa, D. (2019). Understanding the relationship between urban blue infrastructure and land surface temperature. *Science of the Total Environment*, 694, 133742. DOI:10.1016/j.scitotenv.2019.133742

Wu, P., Zhong, K., Wang, L., Xu, J., Liang, Y., Hu, H., Wang, Y. & Le, J. (2022). Influence of underlying surface change caused by urban renewal on land surface temperatures in Central Guangzhou. *Building and Environment*, 215, 108985. DOI:10.1016/j.buildenv.2022.108985

Xiao, X. D., Dong, L., Yan, H., Yang, N. & Xiong, Y. (2018). The influence of the spatial characteristics of urban green space on the urban heat island effect in Suzhou Industrial Park. *Sustainable Cities and Society*, 40, pp. 428-439. DOI:10.1016/j.scs.2018.04.002

Yao, X., Yu, K., Zeng, X., Lin, Y., Ye, B., Shen, X & Liu, J. (2022). How can urban parks be planned to mitigate urban heat island effect in "Furnace cities"? An accumulation perspective. *Journal of Cleaner Production*, 330, 129852. DOI:10.1016/j.jclepro.2021.129852

Zhou, Y., Zhao, H., Mao, S., Zhang, G., Jin, Y., Luo, Y., Huo, W., Pan, Z., An, P. & Lun, F. (2022). Studies on urban park cooling effects and their driving factors in China: Considering 276 cities under different climate zones. *Building and Environment*, 222, 109441. DOI:10.1016/j.buildenv.2022.109441

Zhu, X., Wang, X., Yan, D., Liu, Z. & Zhou, Y. (2019). Analysis of remotely-sensed ecological indexes' influence on urban thermal environment dynamic using an integrated ecological index: a case study of Xi'an, China. *International journal of remote sensing*, 40, 9, pp. 3421-3447. DOI:10.1080/01431161.2018.1547448